Global distribution of far-ultraviolet emission from the highly ionized gas in the Milky Way

2018.08.30

Young-Soo Jo

Young-Soo Jo[1], Kwang-Il Seon[1,2], Kyoung-Wook Min[3], Jerry Edelstien[4], Wonyong Han[1]

[1]Korea Astronomy and Space Science Institute

[2]Astronomy and Space Science Major, Korea University of Science and Technology

[3]Korea Advanced Institute of Science and Technology

[4]University of California, Berkeley

Korea Astronomy and Space Science Institute

1. Introduction

Interstellar Medium

1. In understanding the formation and evolution of galaxies,
   it is essential to study stars and interstellar medium as the elements that make up the galaxy.
2. Particularly, the macroscopic spatial distribution and interaction of interstellar medium, which occupies most of the Milky Way,
   is an important key to reveal the formation and evolutionary processes of the Milky Way.

The discovery of hot gas

1. *Spitzer (1956)* predicted the existence of hot gas far from the Galactic disk by observation of cool clouds.
2. The detection of a soft X-ray background was the first direction of hot gas (*Bowyer, Field, & Mack 1968*).
3. The allsky observation of X-ray emission (*McCammon et al. 1983; Marshall & Clark 1984; Snowden et al. 1997*).

Questions for the hot gas

1. How supernova energy can be effectively transferred from the Galactic plane to halo? (What is the best model?)
2. What is the volume filling fraction of the hot gas in the Milky Way, and how can we estimate?
3. Is the theory (model) consistent with the observation?

Observation of hot gas

1. Far-ultraviolet emission lines from the transient phase gas ($T=10^{4.5}$-$10^{5.5}$ K) is very useful to detect and diagnose the hot gas.
2. The importance of observing the diffuse FUV emission lines has been suggested for the allsky (*Shull & Slavin 1994; Korpela et al. 1998*).
3. Due to the strong extinction and inability of the ground-based observation, allsky survey has not been made before the early of 21st.

In this study…

We used the data of Far-ultraviolet Imaging Spectrograph (*FIMS*) as an all-sky survey mission of FUV spectrum
to study the environment and distribution of hot gas and to verify the hot gas generation models.

2. Data Reduction: (1) Line selection

FIMS (Far-ultraviolet Imaging Spectrograph)

1. Main payload on the first Korean scientific satellite, *STSAT-1*, operated from 2003 to 2005.
2. $\lambda/\Delta\lambda \sim 550$, spatial resolution~5′
3. L-band (1370—1710 Å), S-band (900—1150 Å)
4. It covers about 86% of the sky.

Emission lines

1. Each line represents typical state of ISM.
2. H_2 : molecular clouds of T~1000 K
3. Al II and Si II* : warm neutral/ionized gas of T~8000 K
4. O VI, Si IV, and C IV : transient gas of $T \sim 10^{4.5}$—$10^{5.5}$ K

Selected lines

1. **C IV** : highest signal-to-noise ratio, peak at $T \sim 10^{5.0}$ K (λλ1548,1551)
2. **O VI** : relatively low SNR but important line ($T \sim 10^{5.5}$ K) (λλ1032,1038)

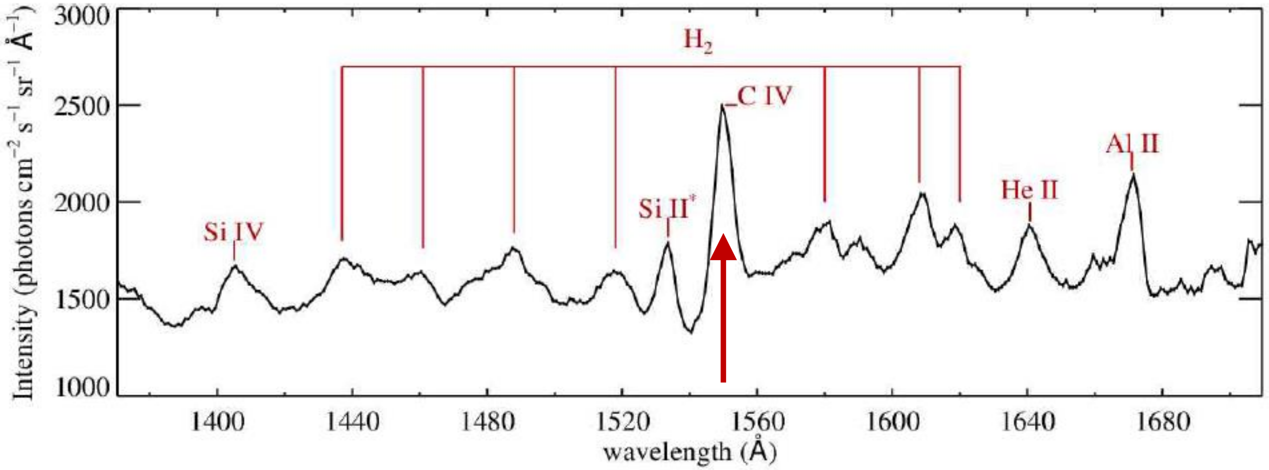

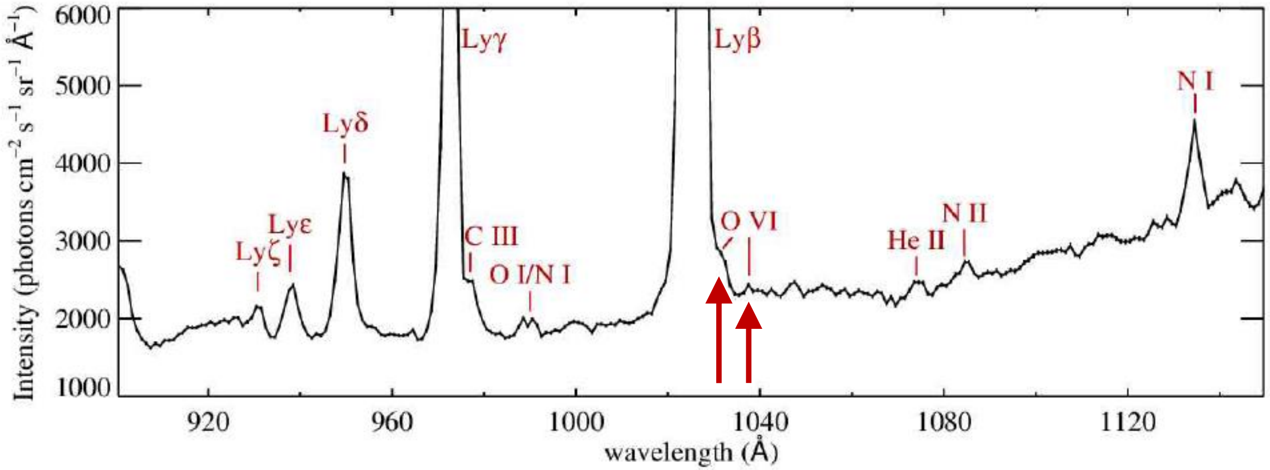

FIMS all-sky spectra averaged over exposure time for the *L*-band (upper) and *S*-band (lower) channels

2. Data Reduction: (2) Fitting of emission lines

1. The intensity of the emission line varies depending on the region,
   an adoptive smoothing method is employed to secure a sufficiently significant signal-to-noise ratio (SNR).

2. The pixel size of the emission map is about 0.92° corresponding to *Nside* = 64 with HEALPix scheme (*Gorski et al. 2005*).

3. The FWHM of the 2D Gaussian kernel as a smoothing kernel varies from 3° to 10° at 0.1° intervals
   to achieve an average SNR>7.0 per wavelength bin of 1 Å size.

2. Data Reduction: (2) Fitting of emission lines

Example spectra for the emission line fittings for the *L*-band (near north Galactic pole region)

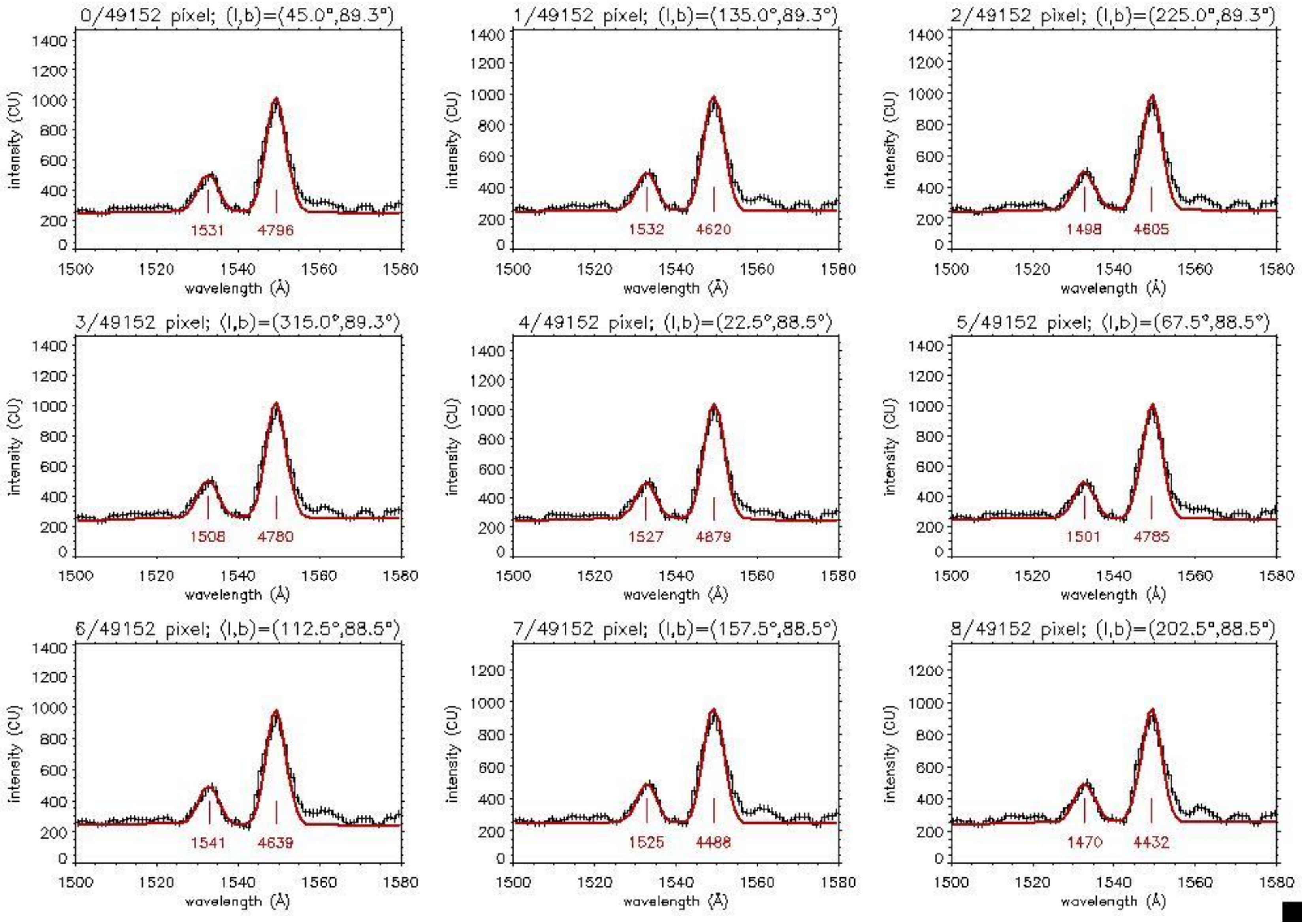

1. Black solid lines:
   observed spectra with error bars
   Red solid lines : model spectra

2. Fitting lines :
   - Si II* (λ1533)
   - C IV (λλ1548, 1551)

3. The red numbers :
   line intensities of Si II* and C IV
   (LU; Line Unit; photons s^{-1} sr^{-1} cm^{-2})

2. Data Reduction: (2) Fitting of emission lines

Example spectra for the emission line fittings for the *S*-band (near Vela supernova remnant region)

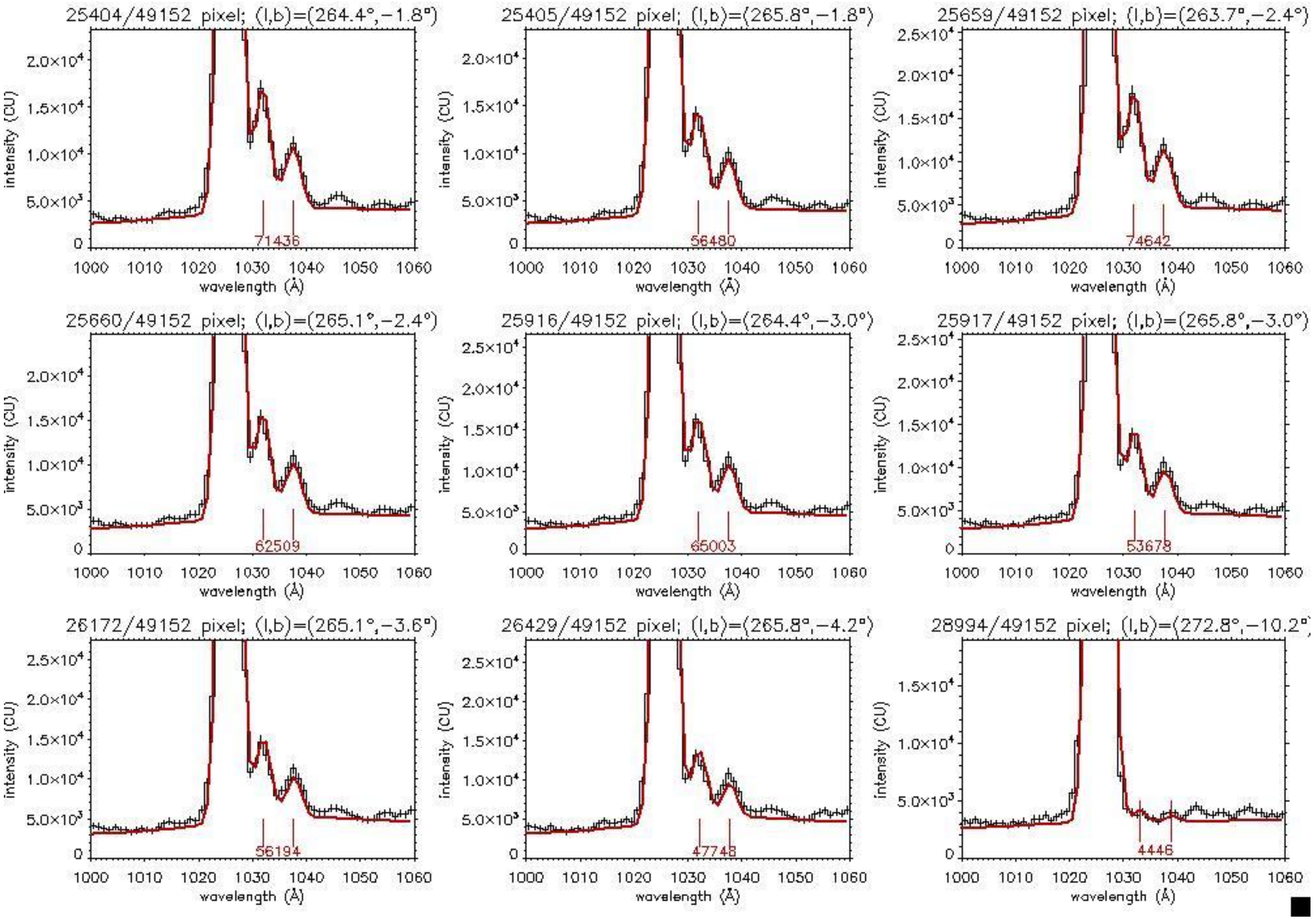

1. Black solid lines:
   observed spectra with error bars
   Red solid lines : model spectra

2. Fitting lines :
   - Lyβ (λ1025)
   - O VI (λλ1032,1038)
   - I(1032)/I(1038) = 2.0

3. The red numbers :
   line intensities of O VI
   (LU; Line Unit; photons s^{-1} sr^{-1} cm^{-2})

2. Data Reduction: (3) All-sky maps of C IV and O VI

Before extinction correction

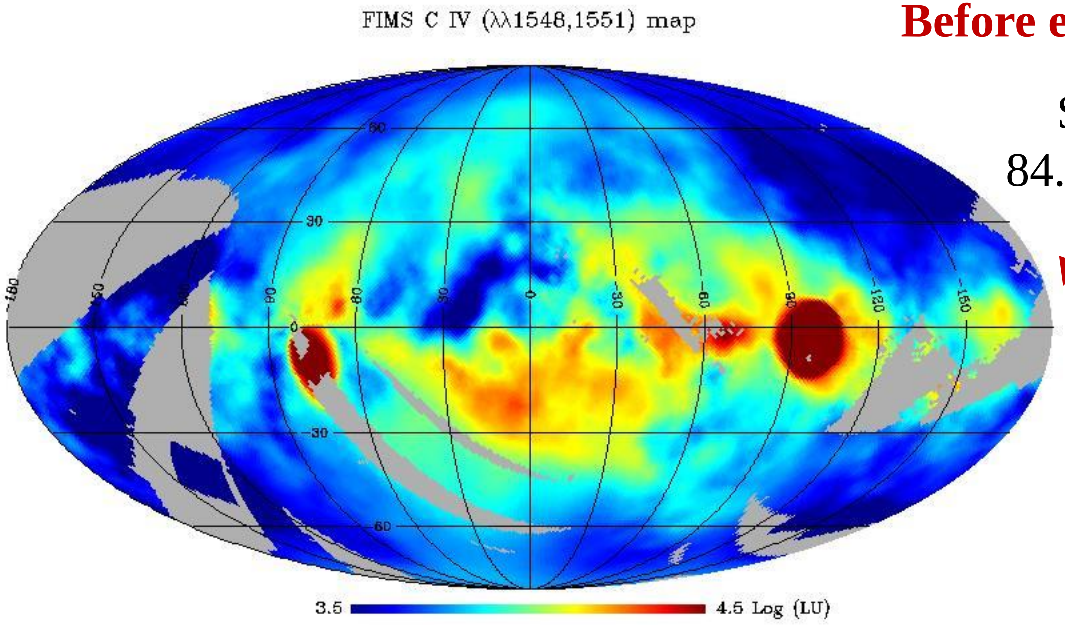

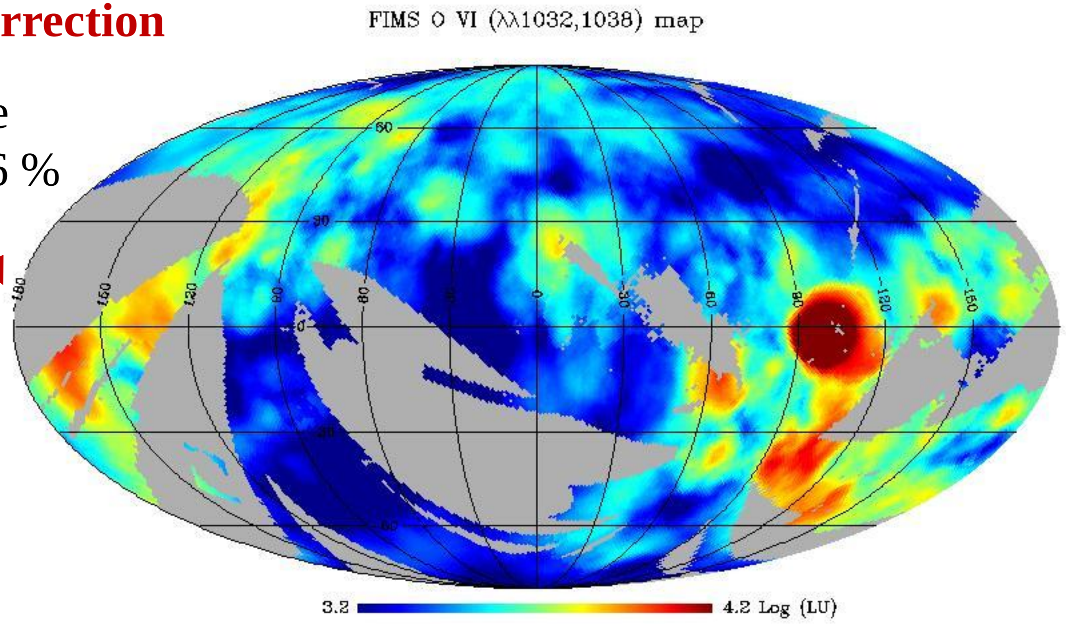

Sky coverage
84.7 % vs 70.6 %

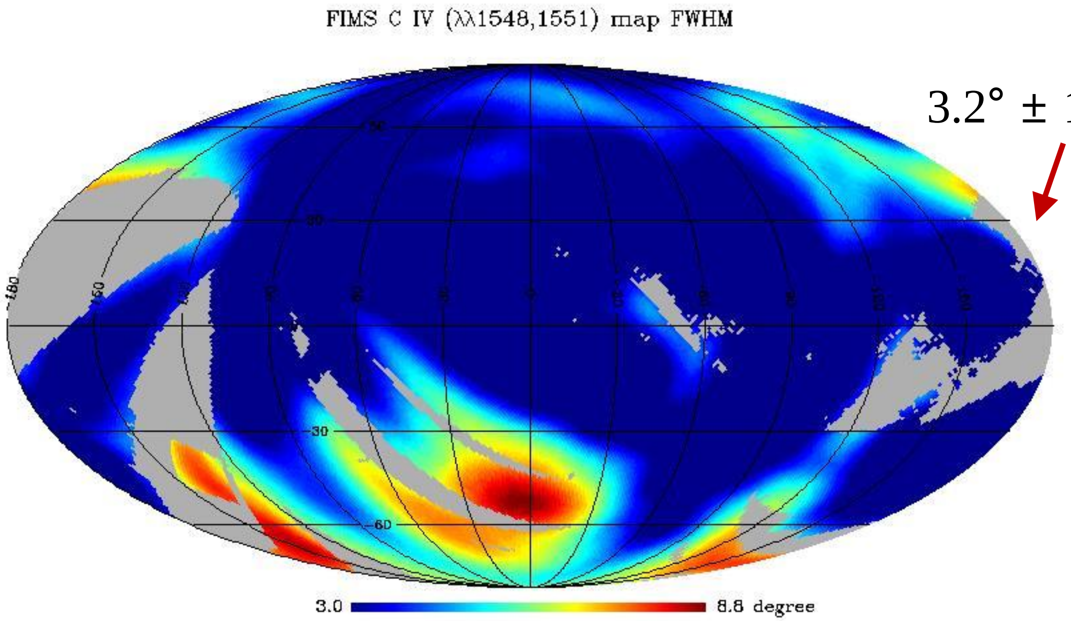

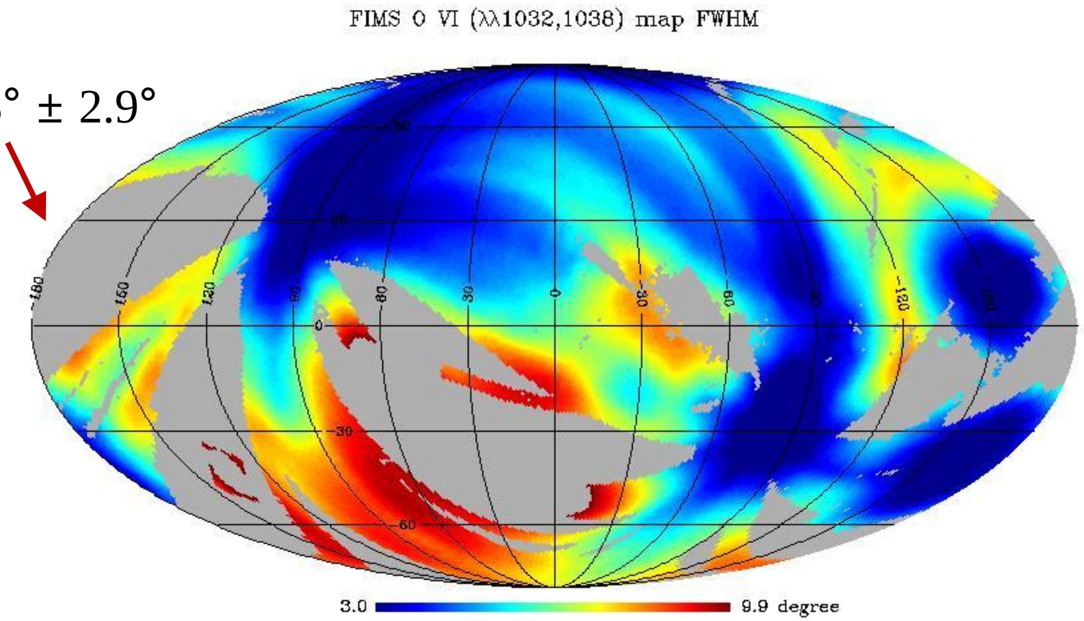

FWHM
3.2° ± 1.8° vs 3.8° ± 2.9°

2. Data Reduction: (4) Extinction correction of the FUV emission maps

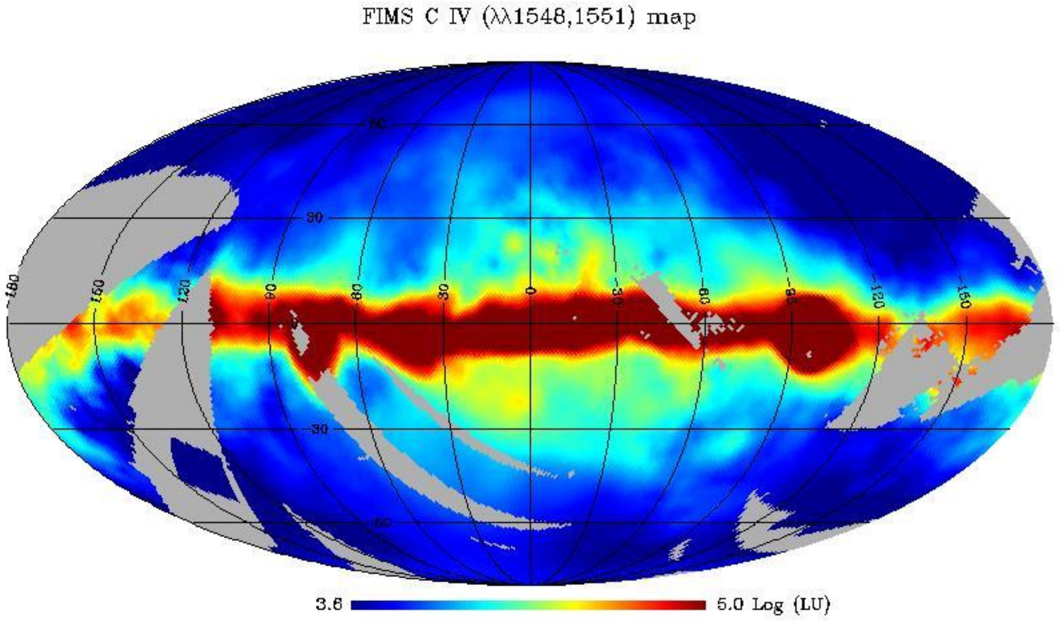

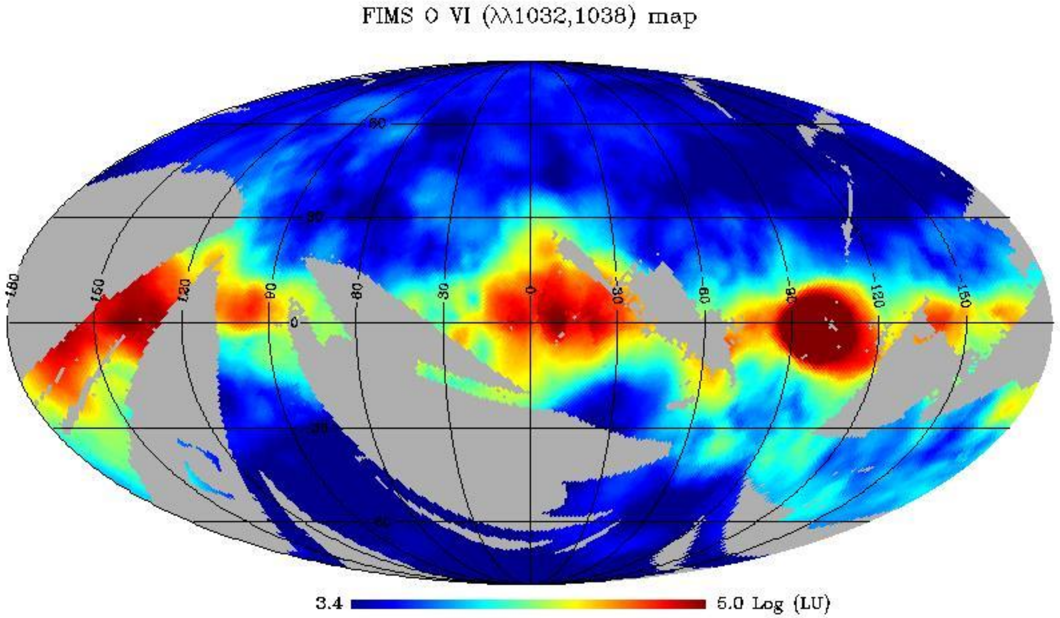

Extinction correction

Assumption : Source and interstellar dust are uniformly mixed.

$$I_{corr} = I \times \frac{\tau}{1 - e^{-\tau}}$$

I : observed intensity
τ :optical depth toward a line-of-sight
I_{corr} : extinction-corrected intensity

Optical depth (τ) : Milky Way extinction curve of for R_V = 3.1, (*Weingartner & Draine 2001*)

$$\tau_{C\ IV} = 7.3\ \times E(B-V)\ at\ \lambda \sim 1550\ \text{Å}$$
$$\tau_{O\ VI} = 11.8\ \times E(B-V)\ at\ \lambda \sim 1035\ \text{Å}$$

The *E(B-V)* map (*Schlegal, Finkbeiner, & Davis 1998*) is convolved with the 2D Gaussian kernels corresponding to the FWHM maps of C IV and O VI.

3. Result: (1) Galactic morphology

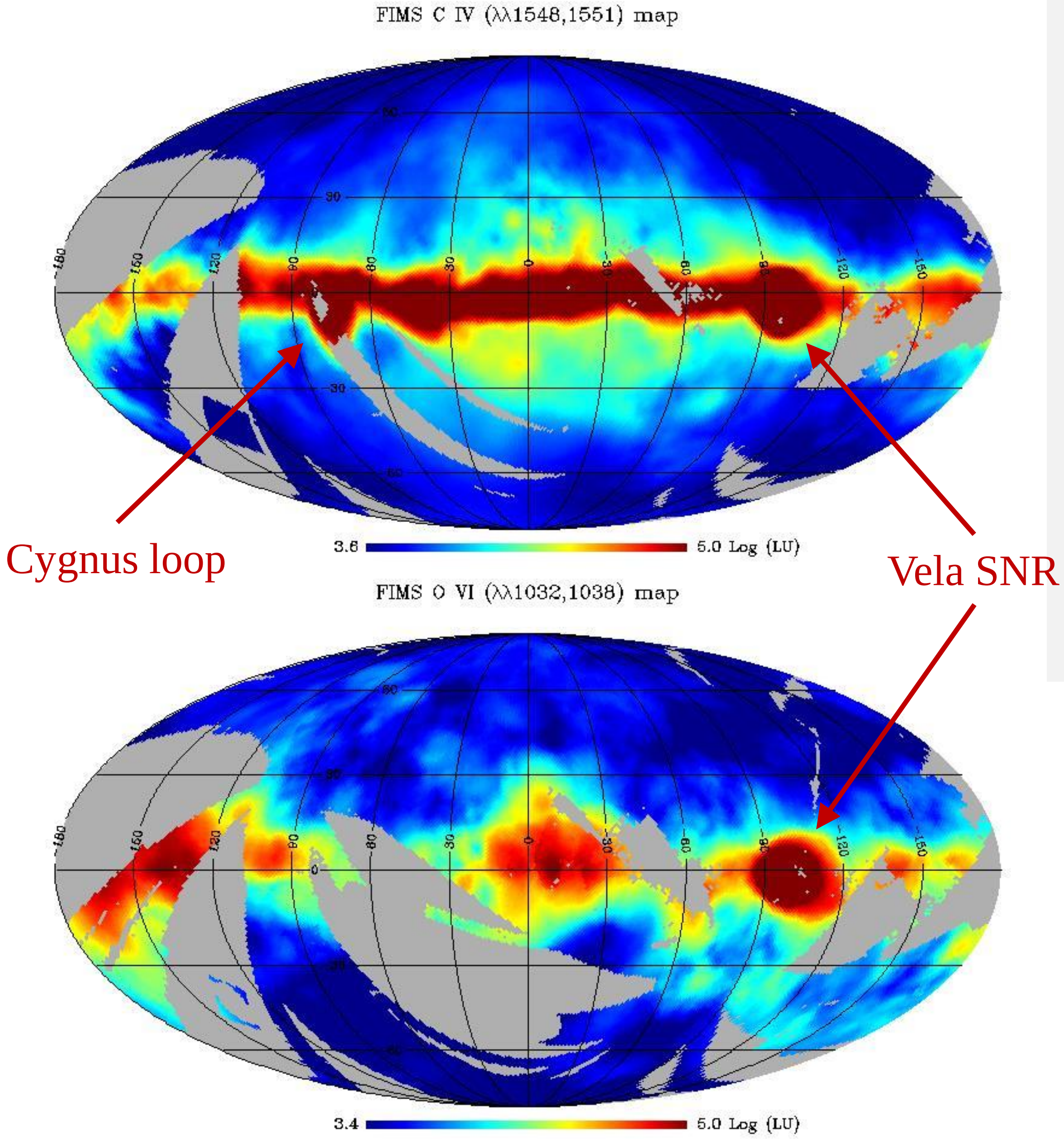

Individual structures

1. The visibility of the FUV emission to the optically thick Galactic plane is limited to about 1 kpc.
2. Therefore, the C IV and O VI emissions being mainly produced by supernova remnants are observed in objects close to the Sun.
   For example, (1) Vela SNR at d~250 pc & at l~-100°,
   (2) Cygnus loop SNR at d~440 pc & l~80°

Large scale structures

Single exponential plane-parallel model

$$\epsilon(z) = \epsilon_0 \cdot \exp\left(-\frac{|z|}{z_0}\right)$$

$$I(\theta) = \int_0^\infty \epsilon(L)dL = \int_0^\infty \epsilon_0 \cdot \exp\left(-\frac{L \cdot \sin|\theta|}{z_0}\right) dL = \frac{\epsilon_0 z_0}{\sin|\theta|}$$

$$I(\theta)\sin|\theta| = \epsilon_0 z_0 = constant$$

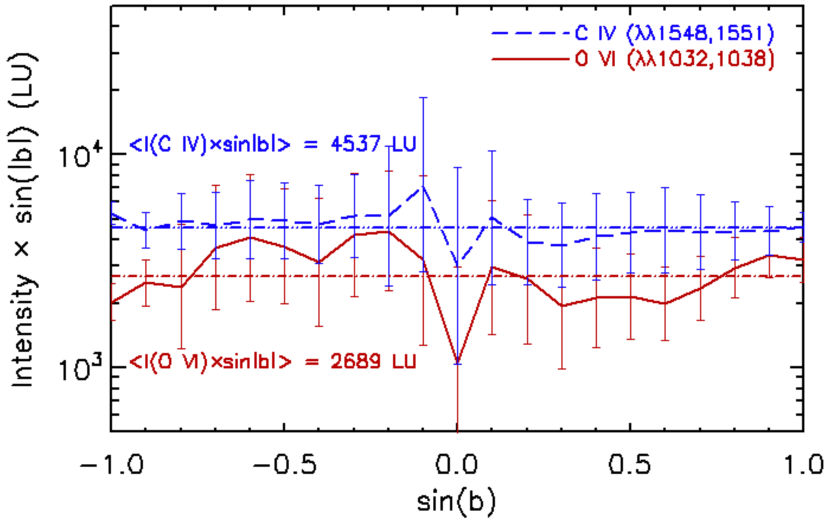

3. Result: (1) Galactic morphology

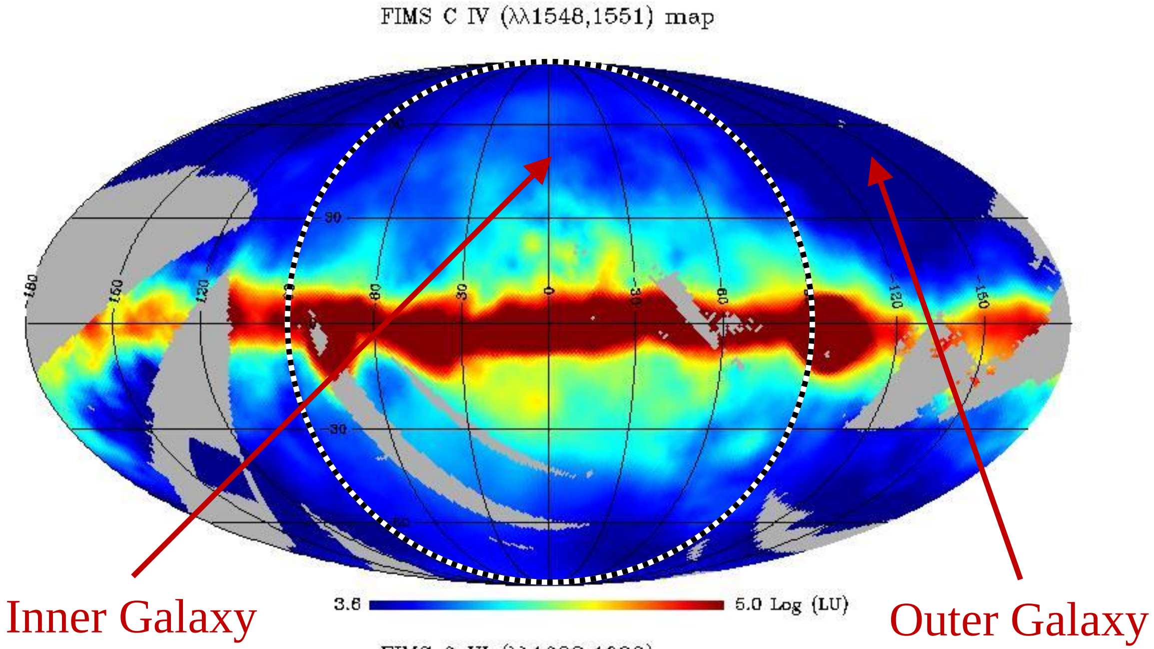

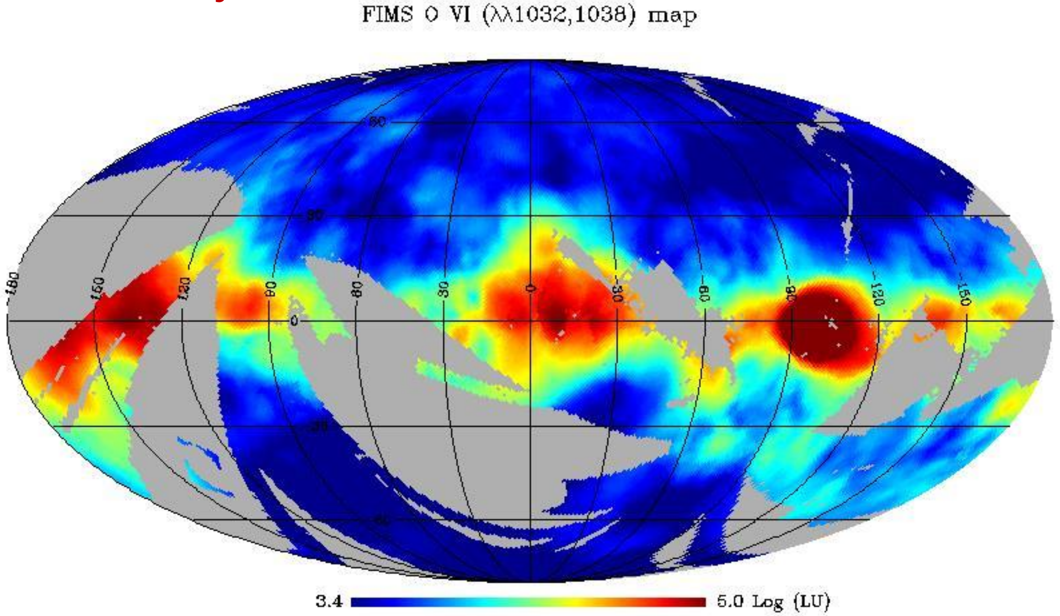

Inner Galaxy vs Outer Galaxy

1. C IV : significant decrease as the Galactic longitude increases.
2. O VI : almost constant. Rather increase as Gal-Lon Increases.

The (relative) galactic morphology of C IV and O VI provides clues to the distribution and state of the transient gas in our galaxy. (ex, Gas temperature, pressure, density, metallicity, interactions…)

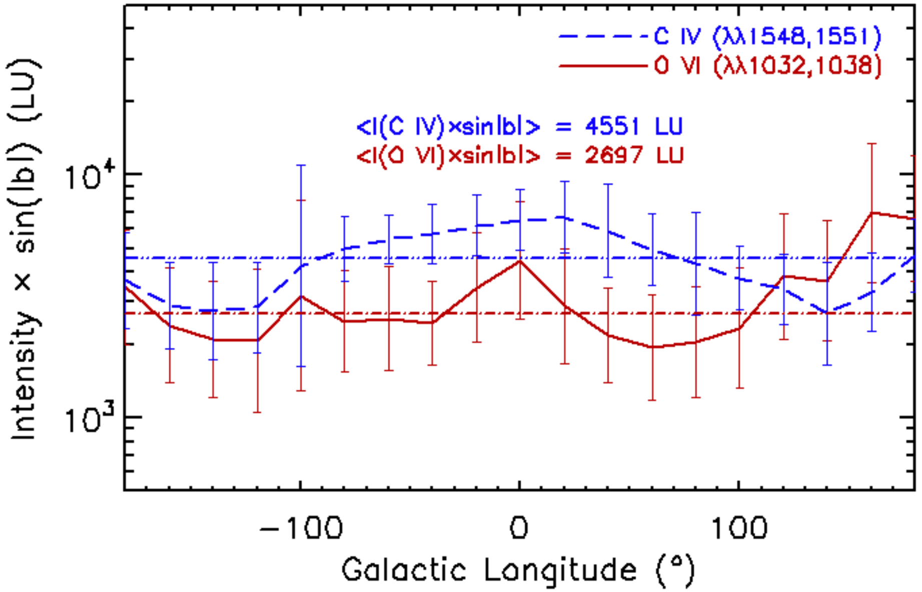

3. Result: (2) Physical properties of the transient gas tranced by C IV and O VI

Assumption : an optically thin and collisionally excited plasma + isothermal plasma of constant density and temperature
Emission measures derived from the observation of C IV and O VI must be same.

$$I_i = \frac{1}{4\pi}\int_0^\infty n_i n_e < \sigma v >_e dx$$

$$= \frac{1}{4\pi}\frac{n_i}{n_H}\frac{n_H}{n_e} < \sigma v >_e \cdot \int_0^\infty n_e^2 dx$$

$$= \frac{1}{4\pi}\frac{n_i}{n_H}\frac{n_H}{n_e} < \sigma v >_e \cdot EM_i$$

$$EM_i = \frac{4\pi\, I_i}{< \sigma v >_e}\frac{n_H}{n_i}\frac{n_e}{n_H} = \frac{I_i}{\gamma_i}\frac{n_H}{n_i}\frac{n_e}{n_H}$$

$$\gamma_{CIV} = 1.09 \times 10^{-8} \cdot T_5^{-0.5} \cdot e^{-\frac{0.929}{T_5}} \cdot \left[\frac{\Omega_{CIV}}{10}\right]$$

$$\gamma_{OVI} = 5.43 \times 10^{-9} \cdot T_5^{-0.5} \cdot e^{-\frac{1.392}{T_5}} \cdot \left[\frac{\Omega_{OVI}}{5}\right]$$

Ω_{CIV} : *Raymond* (1992)
Ω_{OVI} : *Tayal* (2002)
$\frac{n_H}{n_i}$: *Sutherland & Dopita* (1993)

$$n_e = 1.2 n_H$$

At b>60°(at the North Galactic pole region),

$$I(C\,IV)\,sin|b| = 5200 \pm 1100\,(LU)$$
$$I(O\,VI)\,sin|b| = 3200 \pm \ \ 980\,(LU)$$

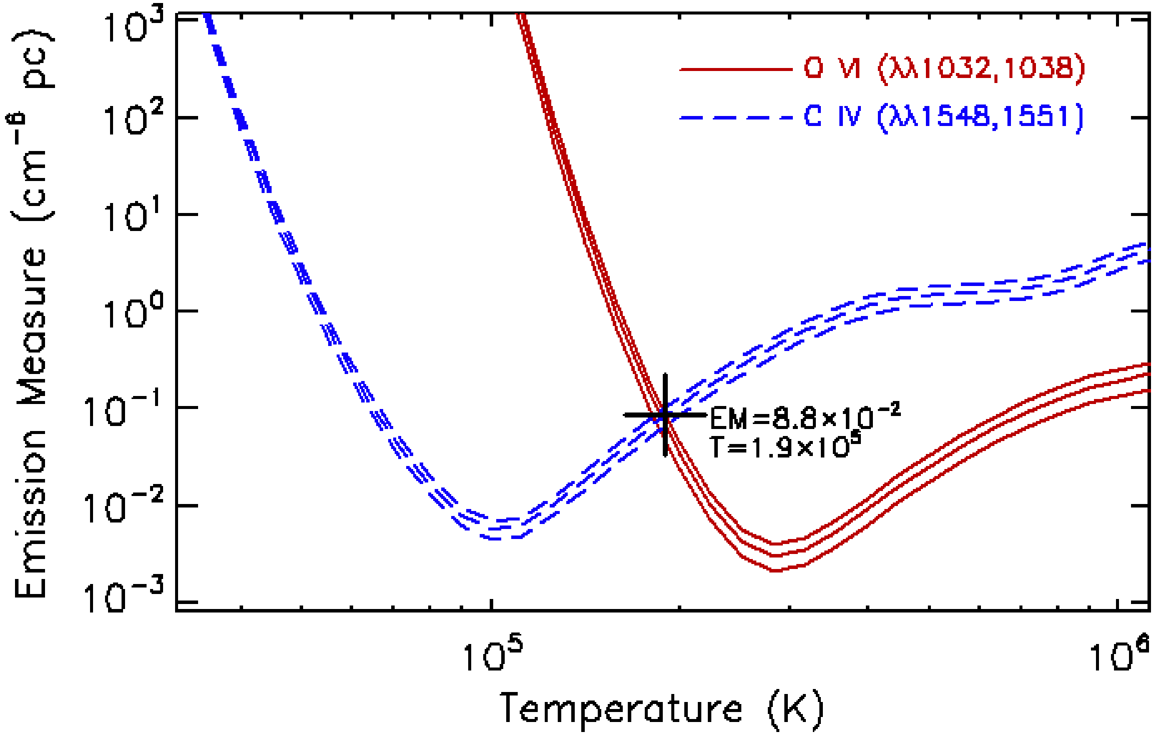

Gas temperature : T~ $(1.9\pm0.1)\times10^5$ K
Emission measure : EM ~ $(8.8\pm0.4)\times10^{-2}$ cm^{-6} pc

3. Result: (2) Physical properties of the transient gas tranced by C IV and O VI

Temperature derived from I(O VI)/I(C IV)

The intensity ratio of C IV and O VI can be written as follows to derive gas temperature.

$$\frac{I_{O\,VI}}{I_{C\,IV}} = \frac{\gamma_{O\,VI}}{\gamma_{C\,IV}} \frac{n_{O\,VI}}{n_{C\,VI}} = \frac{\Omega_{O\,VI}}{\Omega_{C\,IV}} \frac{n_{O\,VI}}{n_{C\,VI}} \cdot e^{-\frac{46,288}{T}}$$

$I_{O\,VI}/I_{C\,IV}$

1. It widely ranges from 0.04 to 6.7.
2. Its median value is 0.63.
3. It is less than 2.0 for more than 94 % of the observed sky.

Gas temperature

1. Despite of the wide variation of $I_{O\,VI}/I_{C\,IV}$, the gas temperature is well defined to $(1.90 \pm 0.09) \times 10^5$ K.
2. Both line ratio and gas temperature are almost constant along Galactic latitude
3. But they tend to increase at the outer galaxy.

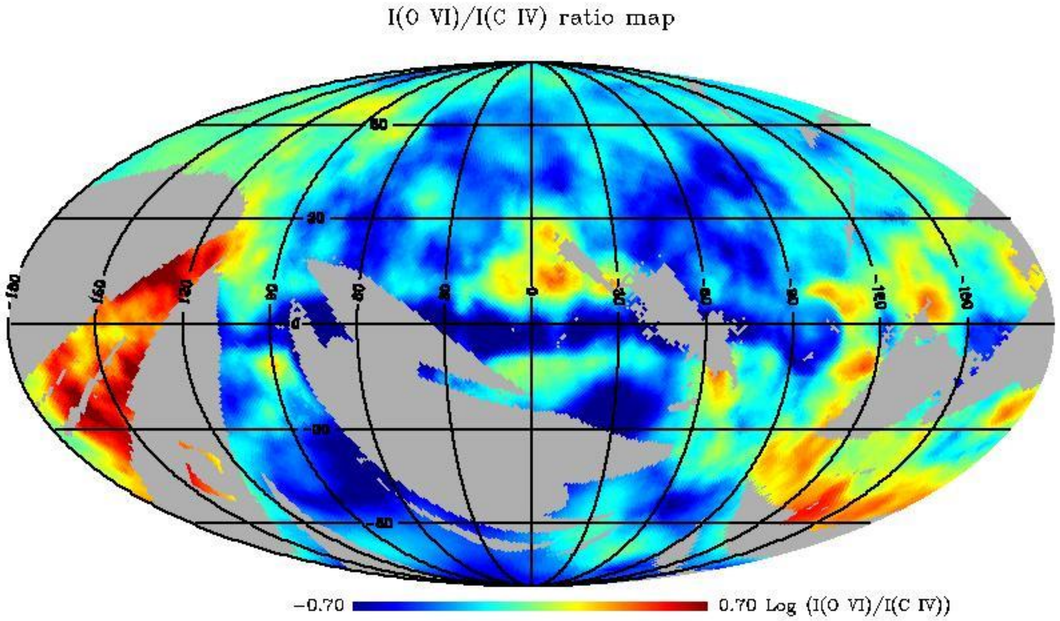

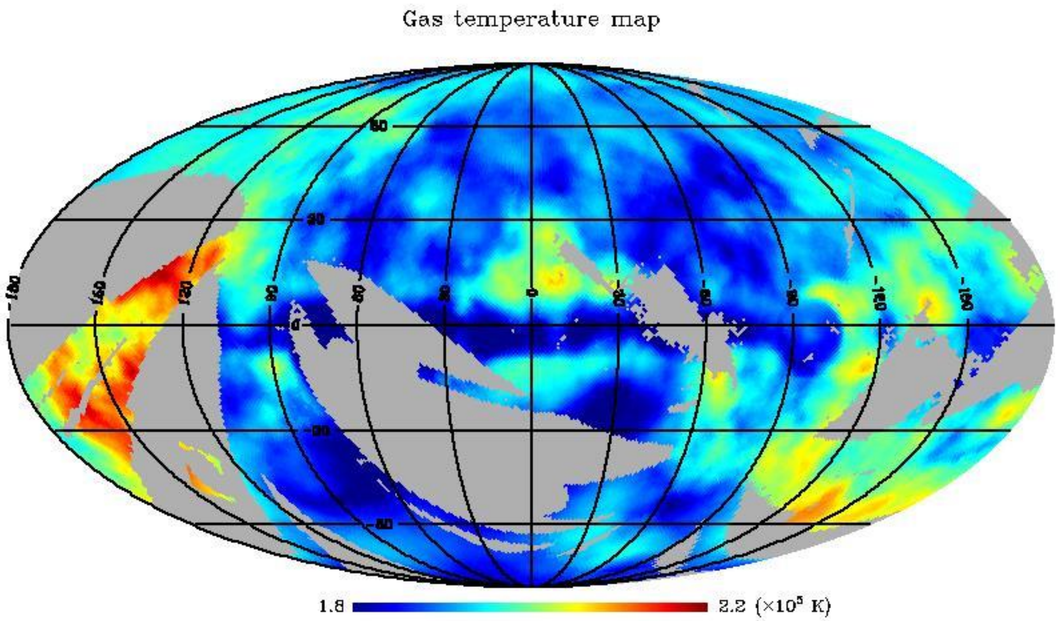

3. Result: (3) Volume filling fraction of the transient gas

$$EM = \int_0^{\infty} n_e^2 dx = n_e^2 L_T$$

$, where\ L_T\ is\ path\ length\ of\ transient\ gas$

$$L_T = \frac{EM}{n_e^2} = \left(\frac{1.92 \cdot T}{P}\right)^2 \cdot EM$$

$(\because P = 1.92\, n_e T\ at\ fully\ ionized\ gas)$

$Definition: Transient\ gas\ volume\ filling\ fraction\ (f)$

$$f = \frac{L_T}{L_{ISM}}$$

$, where\ L_{ISM}\ is\ the\ scale\ height\ of\ C^{+3}\ in\ the\ ISM$

$Let's\ assuming,$

$P = 3000\ cm^{-3}\ K\ (Shull\ \&\ Slavin\ 1994)$

$L_{ISM} = 4.9^{+1.8}_{-1.3}\ kpc\ (Savage\ et\ al.\ 1993; absorption\ line)$

For the north Galactic pole region,

Gas temperature : T~ 1.9×10^5 K

Emission measure : EM ~ 8.8×10^{-2} cm^{-6} pc

$$L_T \sim 1.3\ kpc$$

$$f = \frac{L_H}{L_{ISM}} = \frac{1.3kpc}{4.9kpc} \sim 27^{+9}_{-8}\ \%$$

This large volume filling fraction of transient gas indicates the strong interaction between hot and cold phase gases!!!

Clues to creation and evolution of hot gas in the Milky Way → Compare the observation to the model!!!

3. Result: (4) Hot gas generation models

1. **Isolated supernova-type model** (*Cox & Smith 1974*)
   (1) hot gas volume filling fraction ~ 10%
   (2) Too small predicted I(C IV) ~ 500 LU (cf. observed I(C IV) ~ 5000 LU)
   (3) Too small scale height is required

2. **Three phase models** (*McKee & Ostriker 1977*)
   (1) large hot gas volume filling fraction > 95%
   (1) Still insufficient I(C IV) (*Korpela+ 1998*)

3. **Galactic fountain models** (*Shapiro & Field 1976*)
   (1) Edgar & Chevalier (1986), Houck & Bregman (1990), Shull & Slavin (1994)
   (2) Different prediction of the ratio of *I(O VI)/I(C IV)*

3. Result: (4) Hot gas generation models

1. **Isolated supernova-type model** (*Cox & Smith 1974*)
   (1) hot gas volume filling fraction ~ 10%
   (2) Too small predicted I(C IV) ~ 500 LU (cf. observed I(C IV) ~ 5000 LU)
   (3) Too small scale height is required

2. **Three phase models** (*McKee & Ostriker 1977*)
   (1) large hot gas volume filling fraction > 95%
   (1) Still insufficient I(C IV) (*Korpela+ 1998*)

3. **Galactic fountain models** (*Shapiro & Field 1976*)
   (1) Edgar & Chevalier (1986), Houck & Bregman (1990), Shull & Slavin (1994)
   (2) Different prediction of the ratio of *I(O VI)/I(C IV)*

4. **Galactic fountain model (hybrid model) suggested by *Shull & Slavin (1994)***
   (1) Near the Galactic plane: Isolated SNRs are dominant.
   (2) Galactic halo: Large superbubbles & Turbulent Mixing Layers are dominant.
   (3) Predicted *I(O VI)/I(C IV)=1.2±0.2, I(O IV)=5000—7000 LU*
   (cf. observed I(O VI)/I(C IV)=0.6±0.4, I(O IV)=2200—4200 LU at the North Galactic pole region)

3. Result: (4) Hot gas generation models

1. Isolated supernova-type model (*Cox & Smith 1974*)
2. Three phase models (*McKee & Ostriker 1977*)
3. Galactic fountain models (*Shapiro & Field 1976*)
4. Hybrid model (*Shull & Slavin 1994*)
5. **Recent SNR simulation including superbubbles** (*Joung & Mac Low 2006, Hill et al 2012*):
   Vertical stratification of multi-phase ISM by performing a three-dimensional MHD simulation considering the effect of superbubbles

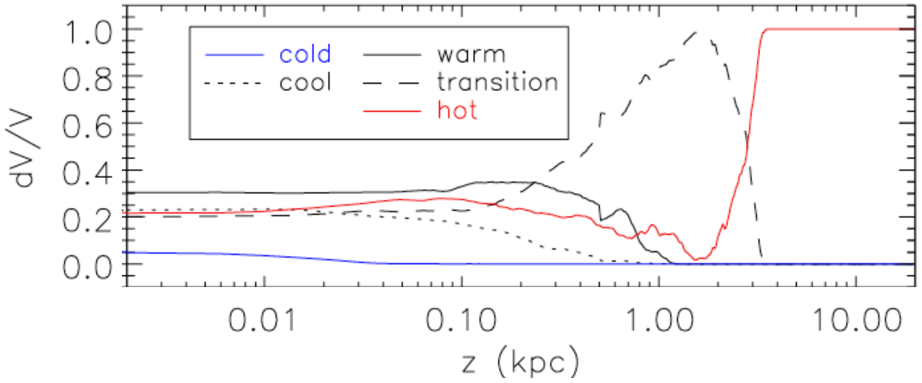

Table 4
Scale Heights of Simulated ISM Components

	Model	Cold		Cool		Warm		Transition		Hot[a]	
		h	n_0	h	n_0	h	n_0	h	n_0	h	n_0
		Exponential fits									
0 μG	bx0hr	8	20	100	0.08	200	0.3	600	0.013	300	0.003
6.5 μG	bx50hr	10	9	90	0.09	190	0.3	600	0.012	500	0.001
13 μG	bx100	11	10	80	0.08	190	0.3	700	0.010	500	0.002

1. Galactic halo is mainly filled with low density hot gas.
2. Transition-temperature gas fills the space at heights $1 \lesssim |z| \lesssim 2$ kpc.
3. The thick transition region is due to the strong interaction between the cold gas in the disk and the hot gas in the halo.
4. Although the transition region decrease as the B-field of ISM increase because of the suppression of turbulent mixing by the field, transition-temperature gas is thick at $|z| \sim 1$ kpc for all cases.

model parameters:
$L_{tran} \sim 1\ kpc$
$EM \sim 5.0 - 7.3 \times 10^{-2}$

observed parameters:
$L_{tran} \sim 1.3\ kpc$
$EM \sim 8.8 \times 10^{-2}$

Consistent result!!!

3. Result: (4) Hot gas generation models

1. Isolated supernova-type model (*Cox & Smith 1974*)
2. Three phase models (*McKee & Ostriker 1977*)
3. Galactic fountain models (*Shapiro & Field 1976*)
4. Hybrid model (*Shull & Slavin 1994*)
5. Recent SNR simulation including superbubbles (*Joung & Mac Low 2006, Hill et al 2012*)
6. **Multiple supernova remnant** (*Vasiliev, Nath & Shchekinov 2015*)

→ The hot gas volume filling fraction and heating efficiency strongly depend on the multiple supernovae much more than isolated single SN.

3. Result: (4) Hot gas generation models

1. Isolated supernova-type model (*Cox & Smith 1974*)
2. Three phase models (*McKee & Ostriker 1977*)
3. Galactic fountain models (*Shapiro & Field 1976*)
4. **Hybrid model** (*Shull & Slavin 1994*)
5. **Recent SNR simulation including superbubbles** (*Joung & Mac Low 2006, Hill et al 2012*)
6. **Multiple supernova remnant** (*Vasiliev, Nath & Shchekinov 2015*)

7. **Conclusion**

   The observation prefers the **hybrid model** given by *Shull & Slavin (1994)*.

   (1) Near the Galactic plane: Isolated SNRs are dominant sources. (ex. Vela, Cygnus loop)

   (2) Hot bubble or hot gas in Galactic halo: Large superbubbles (multiple SNRs) are dominant sources.
   (ex. Orion-Eridanus superbubble, Loop I bubble)

   (3) Large path length of transient gas and EM : strongly mixed regions between plane and halo
   (ex. Turbulent Mixing Layers)

4. Summary

1. We have constructed and analyzed the maps of C IV and O VI emission lines generated from the highly ionized gas to investigate the nature of the Galactic hot gas and to verify the generation models of hot gases.

2. Galactic morphology:
   (1) The C IV and O VI lines are well explained by the simple plane parallel model.
   (The median value of $I \times \sin|b|$ for the C IV and O VI lines are about 4500 LU and 2700 LU, respectively.)
   (2) The C IV intensity decreases from the inner galaxy to the outer galaxy, but the O VI intensity shows the opposite tendency.

3. Environment study:
   (1) Despite of the wide variation of $I_{O\ VI}/I_{C\ IV}$ from 0.04 to 6.7, the gas temperature is well defined to $(1.90 \pm 0.09) \times 10^5$ K.
   (2) The lower gas temperature and higher EM in the inner galaxy may indicate the higher density and pressure, or higher scale height in comparison to outer galaxy.
   (3) Scale length $L \sim 1.3$ kpc and volume filling fraction $f \sim 27\%$ of transient gas toward the north Galactic pole region

4. Hot gas generation model:
   (1) The observations are consistent to the hybrid model combining the isolate supernova-type model to the galactic fountain model.
   (2) Recent MHD simulations also predict the thick transition regions filled with transient gas of $T \sim 10^5$ K indicating the strong interaction between the cold gas in the disk and the hot gas in the halo.
   (3) Both of the simulations and observations imply the important role of superbubbles or multiple SNRs to create the hot gas in the Galactic halo.

Thank you very much